CRYSTAL GROWTH & DESIGN

pubs.acs.org/crystal

Communication

# Gas-Assisted Cocrystal Desublimation

*Published as part of a Crystal Growth and Design virtual special issue in Celebration of the Career of Roger Davey*

Shea Sanvordenker, Siddharth Borsadia, Steve Morris, Naír Rodríguez-Hornedo, and Max Shtein*

Cite This: *Cryst. Growth Des.* 2022, 22, 1528−1532

Read Online



**ABSTRACT:** We report a novel process in which pharmaceutical cocrystals are sublimed, transported by a carrier gas, and directed at high velocity at a substrate, where nano- and microscopic cocrystals are formed. It affords a "touch-free", nonmechanical, single-step means of particle size reduction and surface coating of cocrystals.

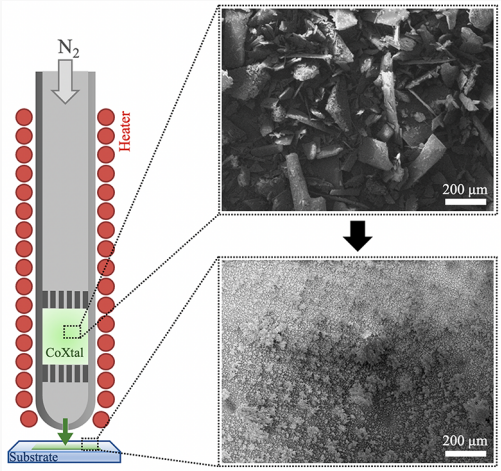


Organic cocrystals are important in pharmaceutical products, energetic materials, foods, and other applications.[1−3] The molecular packing and crystal structure of the cocrystal differ from those of the pure ingredients, often yielding a solubility advantage (SA) when compared to the pure ingredient, i.e., achieving a higher dynamic concentration in a biological system than with a pure form.[4] Different coformers can be employed to make cocrystals of the same active ingredient with different SAs, melting points, and/or mechanical characteristics to meet the potential needs of an application, without modifying the active ingredient's molecular structure (and therefore, biological action mechanism).[5] Guiding principles and methods have been developed for the selection of coformers and creation of cocrystals.[6−11] These approaches have been limited to generating cocrystals in essentially bulk powder form, convenient for crystal structure determination and property assessment but limited in the ability to drastically reduce particle size or create different drug product formats.

Here, we demonstrate a new approach for processing cocrystals in which bulk cocrystals or cocrystal powder is sublimed into a carrier gas and impinged at high velocity onto a cooled substrate. Simple sublimation of cocrystals has been reported in the past;[12−15] yet, control of yield, particle size, and placement were lacking. In this work, a regime is achieved in which both components of the cocrystal desublimate simultaneously, enabling the formation of nano- and microscopic cocrystals *on the target surface*. This gas-assisted process facilitates aseptic processing, a high degree of control over process variables, compatibility with process automation, and continuous manufacturing flow, and by enabling the formation of cocrystalline *coatings* on arbitrary substrates, it greatly minimizes direct drug substance and drug product handling.

Consider the apparatus schematic in Figure 1. A 10 mm diameter steel tube with a 1 mm diameter orifice on the downstream end contained preformed cocrystal, kept at the desired temperature.[16] Nitrogen entered the tube at a rate controlled by a Sierra Instruments Smart-Trak 2 digital mass flow controller, picking up the vapor of the cocrystal and impinging on a cooled borosilicate glass substrate, while the substrate was rastered, as shown. The cocrystals loaded into the apparatus as test-cases consisted of carbamazepine−

**Received:** October 25, 2021
**Revised:** January 28, 2022
**Published:** February 4, 2022







https://doi.org/10.1021/acs.cgd.1c01241
*Cryst. Growth Des.* 2022, 22, 1528−1532

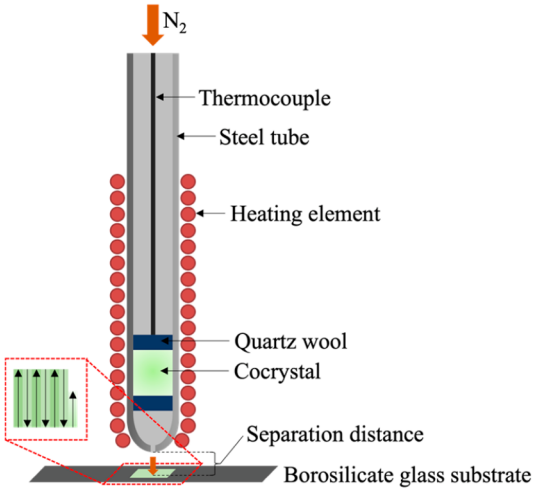


**Figure 1.** Apparatus diagram.

succinic acid (CBZ−SUC) and indomethacin−saccharine (IND−SAC), presynthesized following previously reported procedures using the solvent evaporation method.[17,18] The amount of cocrystal loaded allowed for sufficient mass flow out of the nozzle orifice and for slow depletion during experimentation.

Differential scanning calorimetry (DSC) and thermogravimetric analysis (TGA) were performed on the pure components and on the cocrystal (Figure 2). A TA Instruments DSC Q200 was used with a 40−400 °C heating range and 10 °C per minute heating rate; it was sufficient to collect initial heating curves, without a cooling and secondary heating step. The initial melting peak temperature and enthalpy of melting values for each sample were determined using Universal Analysis software from TA Instruments. A TA Instruments TGA Q500 was used with a 25−400 °C heating range and a 10 °C/min heating rate. Powder was placed into a 5 mm diameter aluminum sample pan, itself placed and centered in a platinum hang pan. Enthalpies of sublimation were determined by fitting a classical Arrhenius behavior model. Key parameters from the TGA and DSC data are summarized in Table 1, which agree with published values for the pure and cocrystal species.[17−20] The TGA curves for both systems show that cocrystals can be vaporized without thermally degrading, with a corresponding preferred range of process temperatures (Table 2).

Unlike in other sublimation-based processes, the entire cocrystal is processed at once, *and* substantially smaller crystals are obtained as the output. For example, scanning electron micrographs (SEMs) (see Figure 3), collected on a JEOL IT500 SEM, clearly show the prevalence of large (>100 $\mu$m) crystallites in bulk synthesized and dried CBZ−SUC; grinding obtains only a slight reduction in size. The material processed here by sublimating the cocrystal whole, followed by transporting the vapors by a carrier gas, followed by direct impingement of the gases onto a cooled substrate, however, yields a coating that exhibits dramatically reduced particle sizes, well below 10 $\mu$m, without any mechanical impaction of the particles during the process.

Powder X-ray diffraction (PXRD) measurements were collected at room temperature (∼300 K), on a Rigaku Miniflex 600 with a CuK$\alpha$ X-ray radiation source ($\lambda$ = 1.54 Å), at a fixed tube voltage of 40 kV and a fixed tube current of 15 mA.

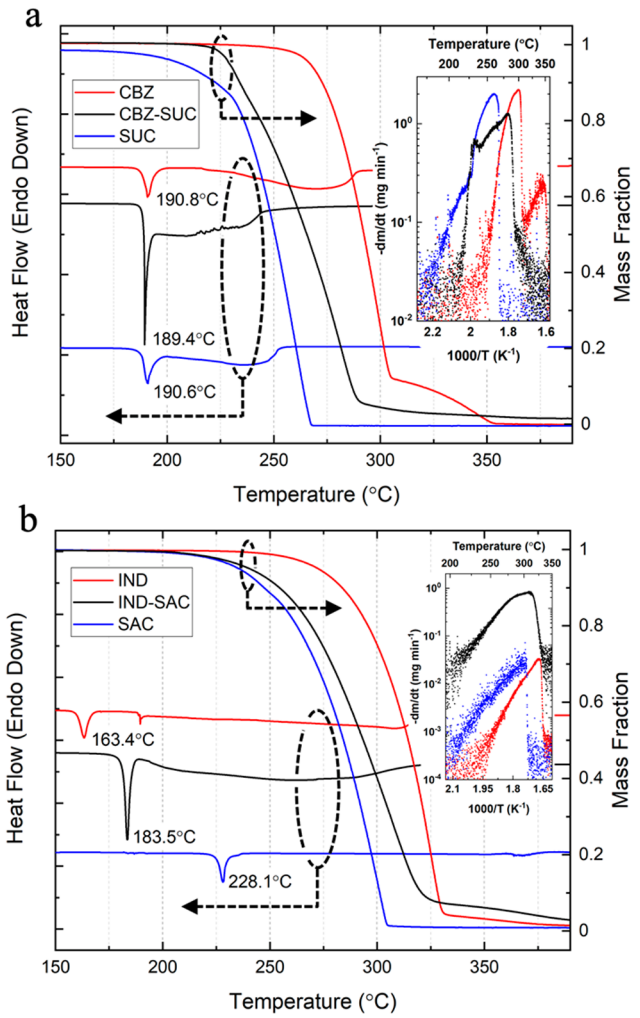


**Figure 2.** TGA and DSC results on APIs, coformers, traditionally formed cocrystal powders for (a) CBZ−SUC and (b) IND−SAC. The insets show Arrhenius type plots (i.e., log(rate) vs $T^{-1}$) which were used to extract the enthalpy of sublimation.

**Table 1. DSC and TGA Results**

| | melting | | | sublimation | | |
|---|---|---|---|---|---|---|
| material | $T_{onset}$ (°C) | $T_{peak}$ (°C) | $\Delta H_{melt}$ (kJ/mol) | $\Delta H_{sub}$ (kJ/mol) | $T_{low}$ (°C) | $T_{high}$ (°C) |
| CBZ | 189.2 | 190.8 | 26.5 | 203.3 | 220 | 280 |
| SUC | 187.9 | 190.6 | 33.0 | 96.5 | 140 | 230 |
| CBZ−SUC | 189.1 | 189.4 | 94.6 | 282.7 | 200 | 230 |
| CBZ−SUC print | | 187.4 | | | | |
| IND | 160.2 | 163.4 | 33.5 | 114.2 | 200 | 320 |
| SAC | 225.4 | 228.1 | 36.3 | 107.0 | 200 | 290 |
| IND−SAC | 181.7 | 183.5 | 73.7 | 102.4 | 200 | 280 |

**Table 2. Process Settings Used to Generate Desublimate**

| process parameter | CBZ−SUC | IND−SAC |
|---|---|---|
| mass loaded (mg) | 100 | 200 |
| cocrystal temperature (°C) | 170 | 200 |
| nitrogen flow rate (SCCM) | 150 | 200 |
| separation distance (mm) | 2 | 4 |
| substrate temperature (°C) | ∼25 | 20 |
| raster velocity (mm/s) | 0.32 | 0.32 |


https://doi.org/10.1021/acs.cgd.1c01241
Cryst. Growth Des. 2022, 22, 1528−1532

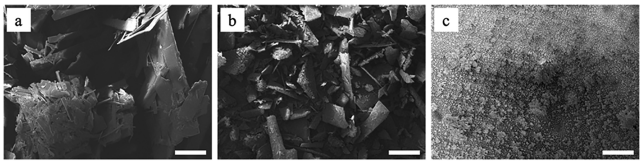


**Figure 3.** SEM of (a) CBZ−SUC cocrystal formed via solvent evaporation, (b) postground in agate mortar, and (c) desublimated CBZ−SUC on glass. 200 $\mu$m scale bar.

Diffraction patterns were recorded for polycrystalline thin films on glass and powders with the beam scanned between 5 and 40° (2$\theta$). Peak positions were compared to known peak positions for pure components and cocrystals to identify the presence of any new crystalline phases after desublimation. The as-deposited films of CBZ−SUC retain the key peaks at 2$\theta$ = 5.8°, 9.7°, 11.5°, 14.7°, 22.8°, and 29.9° previously identified with the cocrystal state (Figure 4a)[17,21] Four new minor peaks appeared as well, corresponding to the desublimated $\beta$ phase of succinic acid (2$\theta$ = 22.1°, 27.2°, 32.5°)[22] and Form I of carbamazepine (2$\theta$ = 28.2°).[23]

As-deposited films of IND−SAC were amorphous but began to convert to cocrystals upon annealing above 60 °C, as PXRD data (Figure 4b) and optical micrographs (Figure 5) show. A cocrystal phase peak at 2$\theta$ = 5.4° appeared above 120 °C.[18] As-deposited SAC remained in the same phase as the powder.

During the process, CBZ−SUC was heated to below its melting point. In contrast, IND−SAC was heated above its melting point to allow for sufficient deposition rates during printing. To determine if the cocrystals melt congruently or incongruently, PXRD was performed on melted and cooled samples. PXRD of melted IND−SAC in Figure 6 indicates it remains a cocrystal once cooled. The characteristic peak at 5.4° is present, as well as all other peaks corresponding to the solvent-evaporated formed cocrystal. This suggests the cocrystal does not separate into individual liquid phases upon melting, therefore indicating that the components volatilize in a stoichiometric ratio. This contrasts with the result of melted and cooled CBZ−SUC, which does not recrystallize into the same phase as indicated in Figure 6. Fortunately, CBZ−SUC remains below the melting temperature during processing, avoiding this potential issue. Additional care should be taken when investigating a cocrystal that must be processed above its melting temperature.

Thermal analysis provides a starting basis to determine the process window for successful cocrystal formation via a desublimation process. The target temperature for the process is preferably in a region where the sublimed active pharmaceutical ingredient (API) and coformer readily remain in the vapor phase. Too low a temperature, and the less volatile compound may desublimate within the heated tube, altering the ratio of API to coformer that will react to form a cocrystal and reaching a cooled surface.[24] Moreover, decreasing temperature reduces the sublimation rate and thus restricts the amount of material that can be processed. The upper temperature limit of the process is largely dictated by the thermal stability of each component. For example, CBZ may begin to decompose appreciably before reaching 180 °C, well below its melting temperature.[25] These factors result in a relatively slim heating window of 160−170 °C for CBZ−SUC. The lower end of this window was determined by analysis of sublimation rates in the experimental apparatus based on initial thermogravimetric analysis. Sublimation rates were found to be higher in the apparatus at heating temperatures identical to the TGA due to a larger amount of material used and convective transport. This allowed for lower temperatures to be used, particularly beneficial in the case of CBZ due to its decomposition well below the sublimation range in the TGA. On the other hand, IND is stable up to 248 °C, well above its melting point.[26] To achieve similar desublimation rates as CBZ−SUC, heating to above the melting point was necessary. The optimal heating range was determined to be 200−225 °C; above 225 °C may be viable as well, as indicated by the linear nature of the Arrhenius plot (i.e., logarithmic mass loss rate versus inverse temperature) in that range (Figure 2b). Different temperature ranges may apply if a different process pressure is used.

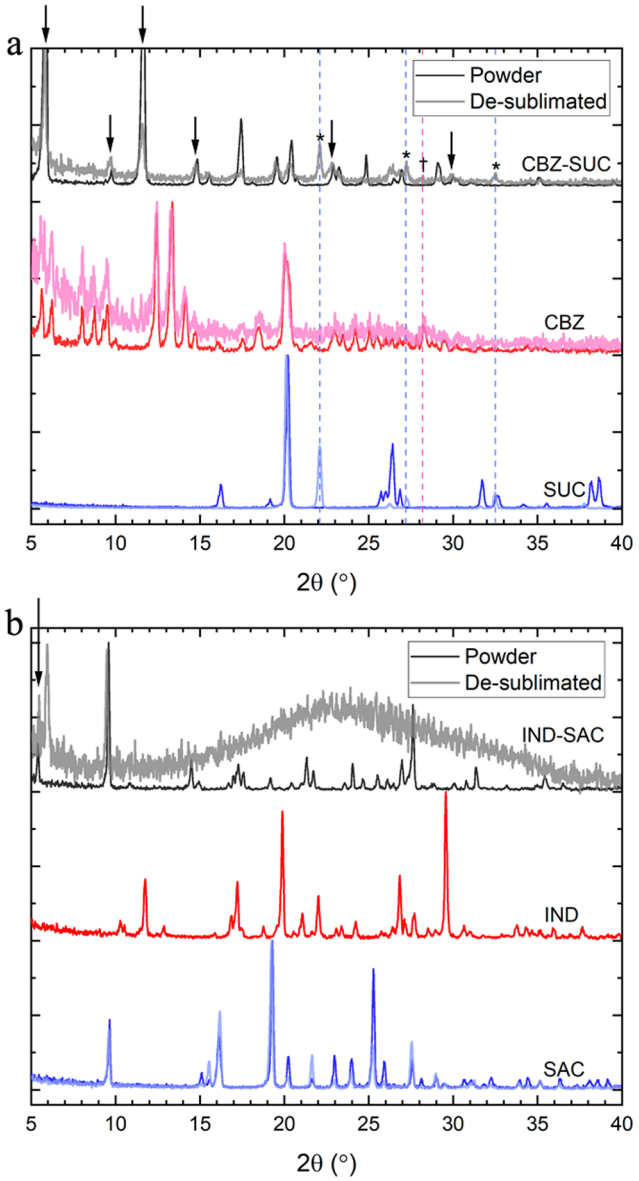


**Figure 4.** PXRD of powder and deposit for (a) CBZ−SUC and (b) IND−SAC systems. Arrows indicate characteristic cocrystal peaks, and stars and dagger correspond to SUC and CBZ peaks, respectively. (Small amounts of non-cocrystallized CBZ and SUC may be present (e.g., peaks at 2$\Theta$ ≈ 17.5, 19.5, 20.5, 24.5°) in conventionally made powder and the desublimated/deposited material.)


https://doi.org/10.1021/acs.cgd.1c01241
Cryst. Growth Des. 2022, 22, 1528−1532

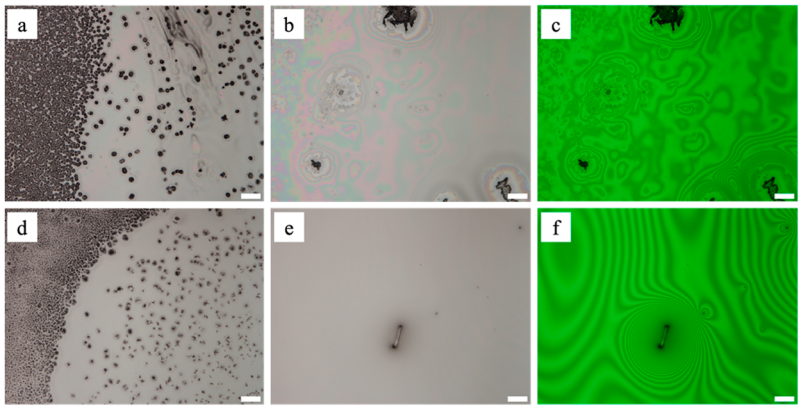


**Figure 5.** Micrographs of IND−SAC desublimate; 1-(a→b): annealing at 60 °C for 1 h, 2-(d→e) at 120 °C for 1 h. Images (c) and (f) were taken with a green light filter. Scale bar: 100 $\mu$m.

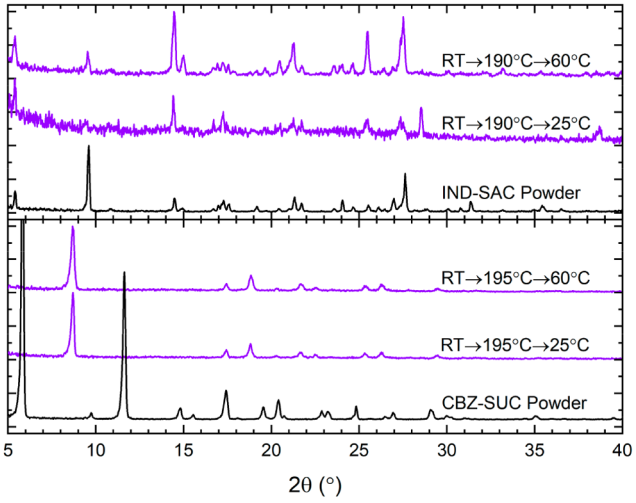


**Figure 6.** PXRD of solvent evaporation-formed cocrystals before and after heating to 5 °C above the melt and cooling to 25 or 60 °C. Isotherms were held for 10 min, and the heating/cooling rate was 10 °C per minute.

Substrate temperature also plays an important role in successful cocrystal desublimation. For CBZ−SUC, the cocrystal was formed with the substrate held above room temperature, but less success was observed for colder substrates (e.g., 10 and 25 °C); IND−SAC was found to desublimate into an amorphous solid, requiring an annealing step to crystallize into IND−SAC. A broader range of substrate temperature control may be advantageous for achieving single-step desublimation of cocrystals with behavior similar to the IND−SAC cocrystal.

We have shown here a route for creating organic cocrystal coatings consisting of micron-size cocrystals through a "touch-free", gas flow-assisted, vapor-based approach, without the need for any mechanical grinding or solvents in the formation of the coating. The process conditions and apparatus dimensions are well controlled and suggest that the process and its output are highly scalable. This technique opens the door to single-step processing and deposition of cocrystal systems to broaden the choice of feasible drug delivery applications.

## ■ AUTHOR INFORMATION

### Corresponding Author

**Max Shtein** − *Department of Materials Science and Engineering, University of Michigan, Ann Arbor, Michigan 48109-2800, United States*; orcid.org/0000-0003-4844-5108; Email: mshtein@umich.edu

### Authors

**Shea Sanvordenker** − *Department of Materials Science and Engineering, University of Michigan, Ann Arbor, Michigan 48109-2800, United States*

**Siddharth Borsadia** − *Department of Materials Science and Engineering, University of Michigan, Ann Arbor, Michigan 48109-2800, United States*

**Steve Morris** − *Department of Materials Science and Engineering, University of Michigan, Ann Arbor, Michigan 48109-2800, United States*

**Naír Rodríguez-Hornedo** − *Department of Pharmaceutical Sciences, University of Michigan, Ann Arbor, Michigan 48109-1065, United States*

Complete contact information is available at: https://pubs.acs.org/10.1021/acs.cgd.1c01241

### Notes

The authors declare the following competing financial interest(s): A patent application has been submitted by the University of Michigan.

## ■ ACKNOWLEDGMENTS

We thank Taylor Repetto and Drs. Ronald Larson, Anish Tuteja, and Geeta Mehta for helpful discussions. The authors acknowledge the financial support of this work by NSF Grant 2029139.

## ■ REFERENCES

(1) Shan, N.; Zaworotko, M. J. The role of cocrystals in pharmaceutical science. *Drug Discovery Today* **2008**, *13* (9−10), 440−446.

(2) Schultheiss, N.; Bethune, S.; Henck, J.-O. Nutraceutical cocrystals: utilizing pterostilbene as a cocrystal former. *CrystEngComm* **2010**, *12* (8), 2436.

(3) Bolton, O.; Matzger, A. J. Improved Stability and Smart-Material Functionality Realized in an Energetic Cocrystal. *Angew. Chem., Int. Ed.* **2011**, *50* (38), 8960−8963.

(4) Good, D. J.; Rodríguez-Hornedo, N. Solubility Advantage of Pharmaceutical Cocrystals. *Cryst. Growth Des.* **2009**, *9* (5), 2252−2264.
(5) Duggirala, N. K.; Perry, M. L.; Almarsson, Ö.; Zaworotko, M. J. Pharmaceutical cocrystals: along the path to improved medicines. *Chem. Commun.* **2016**, *52* (4), 640−655.
(6) Wood, P. A.; Feeder, N.; Furlow, M.; Galek, P. T. A.; Groom, C. R.; Pidcock, E. Knowledge-based approaches to co-crystal design. *CrystEngComm* **2014**, *16* (26), 5839.
(7) Friščić, T.; Jones, W. Recent Advances in Understanding the Mechanism of Cocrystal Formation via Grinding. *Cryst. Growth Des.* **2009**, *9* (3), 1621−1637.
(8) Karimi-Jafari, M.; Padrela, L.; Walker, G. M.; Croker, D. M. Creating Cocrystals: A Review of Pharmaceutical Cocrystal Preparation Routes and Applications. *Cryst. Growth Des.* **2018**, *18* (10), 6370−6387.
(9) Perlovich, G. L. Thermodynamic characteristics of cocrystal formation and melting points for rational design of pharmaceutical two-component systems. *CrystEngComm* **2015**, *17* (37), 7019−7028.
(10) Childs, S. L.; Stahly, G. P.; Park, A. The Salt−Cocrystal Continuum: The Influence of Crystal Structure on Ionization State. *Mol. Pharmaceutics* **2007**, *4* (3), 323−338.
(11) Rodríguez-Hornedo, N.; Nehm, S. J.; Seefeldt, K. F.; Pagán-Torres, Y.; Falkiewicz, C. J. Reaction Crystallization of Pharmaceutical Molecular Complexes. *Mol. Pharmaceutics* **2006**, *3* (3), 362−367.
(12) Alsirawan, M. B.; Lai, X.; Prohens, R.; Vangala, V. R.; Shelley, P.; Bannan, T. J.; Topping, D. O.; Paradkar, A. Mecha-nistic Understanding of Competitive Destabilization of Carbam-azepine Co-crystals under Solvent Free Conditions. *Cryst. Growth Des.* **2020**, *20* (9), 6024−6029.
(13) O'Malley, C.; Erxleben, A.; Kellehan, S.; Mcardle, P. Unprecedented morphology control of gas phase cocrystal growth using multi zone heating and tailor made additives. *Chem. Commun.* **2020**, *56* (42), 5657−5660.
(14) Zhang, T.; Yu, Q.; Li, X.; Ma, X. Preparation of 2:1 urea-succinic acid cocrystals by sublimation. *J. Cryst. Growth* **2017**, *469*, 114−118.
(15) Lombard, J.; Haynes, D. A.; le Roex, T. Assessment of Co-sublimation for the Formation of Multicomponent Crystals. *Cryst. Growth Des.* **2020**, *20* (12), 7840−7849.
(16) Shalev, O.; Raghavan, S.; Mazzara, J. M.; Senabulya, N.; Sinko, P. D.; Fleck, E.; Rockwell, C.; Simopoulos, N.; Jones, C. M.; Schwendeman, A.; Mehta, G.; Clarke, R.; Amidon, G. E.; Shtein, M. Printing of small molecular medicines from the vapor phase. *Nat. Commun.* **2017**, *8*, 711.
(17) Childs, S. L.; Rodríguez-Hornedo, N.; Reddy, L. S.; Jayasankar, A.; Maheshwari, C.; Mccausland, L.; Shipplett, R.; Stahly, B. C. Screening strategies based on solubility and solution compo-sition generate pharmaceutically acceptable cocrystals of car-bamazepine. *CrystEngComm* **2008**, *10* (7), 856.
(18) Basavoju, S.; Boström, D.; Velaga, S. P. Indomethacin−Saccharin Cocrystal: Design, Synthesis and Preliminary Pharma-ceutical Characterization. *Pharm. Res.* **2008**, *25* (3), 530−541.
(19) Rahman, F. A.; Rahim, S. A.; Chou, C. T.; Low, S. H.; Ramle, N. A. Carbamazepine-Fumaric Acid and Carbamazepine-Succinic Acid Co-crystal Screening Using Solution Based Method. *International Journal of Chemical Engineering and Applications* **2017**, *8* (2), 136−140.
(20) Fulias, A.; Vlase, G.; Vlase, T.; Suta, L.-M.; Soica, C.; Ledeti, I. Screening and characterization of cocrystal formation be-tween carbamazepine and succinic acid. *J. Therm. Anal. Calorim.* **2015**, *121* (3), 1081−1086.
(21) Ullah, M.; Hussain, I.; Sun, C. C. The development of carbamazepine-succinic acid cocrystal tablet formulations with improved in vitro and in vivo performance. *Drug development and industrial pharmacy.* **2016**, *42* (6), 969−976.
(22) Yu, Q.; Dang, L.; Black, S.; Wei, H. Crystallization of the polymorphs of succinic acid via sublimation at different temperatures in the presence or absence of water and isopropanol vapor. *J. Cryst. Growth* **2012**, *340* (1), 209−215.
(23) Rustichelli, C.; Gamberini, G.; Ferioli, V.; Gamberini, M.; Ficarra, R.; Tommasini, S. Solid-state study of polymorphic drugs: carbamazepine. *J. Pharm. Biomed. Anal.* **2000**, *23* (1), 41−54.
(24) Manin, A. N.; Voronin, A. P.; Manin, N. G.; Vener, M. V.; Shishkina, A. V.; Lermontov, A. S.; Perlovich, G. L. Salicylamide Cocrystals: Screening, Crystal Structure, Sublimation Thermo-dynamics, Dissolution, and Solid-State DFT Calculations. *J. Phys. Chem. B* **2014**, *118* (24), 6803−6814.
(25) Dołega, A.; Zieliński, P. M.; Osiecka-Drewniak, N. New Insight Into Thermodynamical Stability of Carbamazepine. *J. Pharm. Sci.* **2019**, *108* (8), 2654−2660.
(26) Rusu, M.; Olea, M.; Rusu, D. Kinetic study of the indomethacin synthesis and thermal decomposition reactions. *J. Pharm. Biomed. Anal.* **2000**, *24* (1), 19−24.





https://doi.org/10.1021/acs.cgd.1c01241
*Cryst. Growth Des.* 2022, 22, 1528−1532